BMC Plant Biology

RESEARCH

Open Access

Transcriptomic analysis of *Phytophthora infestans* races and evaluation of their pathogenicity on potato

Linmei Deng[1], Jianjun Hao[2], Jiawen Feng[3], Jing Zhao[1], Jian Dao[1], Gaihuan Xu[1], Kunyan Zhou[1], Yajin Xu[1], Wenping Wang[1], Shunhong Zhang[1], Chunjiang Liu[1], Meng Chen[1], Yanli Yang[1*] and Xia Liu[1*]

Abstract

Phytophthora infestans causes potato late blight and significantly impacts potato production. The pathogen's remarkable adaptability and ability to generate new physiological races through virulence variation undermine varietal resistance, posing challenges for disease prevention and control. To explore the genetic mechanisms behind these, different physiological races of *P. infestans* were inoculated on potato leaves and assayed through transcriptomics combined with metabolic profiling methods. It was found that the DL04 strain, which carries virulence factor 3, exhibited a high level of pathogenicity. Biologically, DL04 showed more rapid growth and denser mycelial structures compared to most other strains, indicating enhanced pathogenicity. DL04 induced a greater enrichment of carbon metabolism, biosynthesis of amino acids, and glycolysis/gluconeogenesis pathways during the infection process. This led to the upregulation of genes related to cell hydrolysis, accelerating leaf infection and contributing to its higher level of pathogenicity. The reasons for the differences in pathogenicity among different physiological races of *P. infestans* were clarified at the transcriptional level. This finding provides valuable insights into the genetic basis of *P. infestans* pathogenicity and offer critical information for developing effective control strategies, breeding for disease resistance, and improving potato production practice.

Keywords Physiological races, Genetic analysis, Late blight, Metabolic pathways, Potato resistance

Introduction

Late blight caused by *Phytophthora infestans* is the most devastating disease of potato (*Solanum tuberosum*) [1]. Potatoes have developed multiple late blight resistance genes. Currently, 11 resistance genes (*R1-R11*) have been identified in potatoes, each counteracting a corresponding *P. infestans* race and virulence factor. However, *P. infestans* continually evolves new physiological races that overcome the host resistance. Conventionally, *P. infestans* races are determined using a set of indicator potato varieties, each of which harboring one of the known resistance genes [2]. However, the rapid emergence of novel *P. infestans* races is outpacing the development of resistant

*Correspondence:
Yanli Yang
yangyanliyyl@foxmail.com
Xia Liu
liuxia_0213@163.com
[1]Key Laboratory for Agro-biodiversity and Pest Control of Ministry of Education, College of Plant Protection, Yunnan Agricultural University, Kunming 650201, China
[2]School of Food and Agriculture, The University of Maine, Orono 04469, ME, U.S.A.
[3]Agricultural and Rural Bureau, Qujing 655199, China

varieties [3–5], leading to the breakdown of resistance mechanisms.

Virulence factor 3 has been identified as a key determinant of pathogenicity in *P. infestans*, multiple studies worldwide have emphasised the necessity of investigating the impact of epidemic races on the severity of potato late blight [6–8]. A total number of 126 *P. infestans* isolates from Poland were analysed and found *vir3* present in 99% of strains, all of which exhibited resistance to R3 host plants [9]. A total number of 116 *P. infestans* isolates from Latvia were analysed that more than 80% of the isolates were resistant to R3 [10]. Virulence gene analysis of *P. infestans* physiological races in Fujian, China, found that 100% of the strains carried *vir3* [11]. Similarly, virulence factor 3 and virulence factor 4 to be predominant in Sichuan, China [12]. Furthermore, the dominance frequency of virulence factor 3 in up to 91.7% of collected strains [13], reinforcing the virulence factor 3 central role in the pathogenic virulence. This widespread prevalence has resulted in the complete loss of resistance in potato cultivars containing the major *R3* resistance gene.

Transcriptome sequencing plays an important role in the study of plant responses to pathogen-induced stress, unraveling the pathogenic mechanisms of plant pathogens [14], and contributing to understanding the interaction between pathogens and plant hosts [15]. RNA sequence (RNA-seq) effectively evaluates key pathogen-host interaction genes, elucidating molecular mechanisms of pathogenesis [16], and enables rapid identification of upregulated pathogen effector genes during early infection [17, 18]. For example, The dynamics of metabolism, signaling and virulence genes of *P. infestans* strains at different developmental stages during the mycelium-sporangium transition have significant changes [19]. Similarly, In response to the production of phenazine-1-carboxylic acid (PCA) by *Pseudomonas fluorescens*, the expression of key functional genes such as PCA-induced phosphorylation, transmembrane transport and redox activity was significant [20]. The transcriptional response process of potato leaves and tubers after inoculation with *P. infestans* showed that significant differences in the responses of leaves versus tubers, but noted that core genes related to defense were highly upregulated in both tissues [21]. These findings provide a new way for the prevention and control of plant diseases, and a theoretical basis for the screening of host resistance genes.

Traditional plant disease studies assess pathogenicity through phenotypic and biochemical traits, yet lacks accuracy in predicting dynamic pathogenicity changes of *P. infestans.* Transcriptomic profiling overcomes these limitations by sensitively detecting pathogenesis-associated genes and pathways, enabling comprehensive host-pathogen interaction analysis. This study integrates phenotypic characterization with transcriptomics across distinct *P. infestans* physiological races to unravel virulence gene-driven mechanisms underlying pathogenic variations during potato infection.

Table 1 *Phytophthora infestans* strains used in this study

Strain number	Physiological races / Virulence factor
MLS13418-2	8.10
NLL605	10.11
ZTQ907	1.3.11
MLS13418-1	1.2.4.5.10
HS03	3.6.8.10.11
XDL601	1.2.4.5.9.11
DQ01	1.2.3.4.5.10
JAX207	1.2.3.4.5.6.11
LJ05	1.2.3.4.5.10.11
HS02	2.4.5.6.8.10.11
DSPQ006	1.2.4.5.6.8.10.11
ML01-2018	1.2.3.4.5.9.10.11
XDQ901	1.2.3.4.5.8.9.10.11
HZ02	1.2.4.5.6.8.9.10.11
LJ04	1.2.5.6.7.8.9.10.11
ML01-2019	1.2.3.4.5.6.7.8.9.10
DL04	1.2.3.4.5.6.8.9.10.11
JCZ29	1.2.3.4.5.6.7.8.10.11
MLS8802	2.3.4.5.6.7.8.9.10.11
HJG02	1.2.3.4.5.6.7.8.9.10.11

Materials and methods

Phytophthora infestans strains

Twenty physiological races of *Phytophthora infestans* were isolated from potato leaves showing late blight symptoms in Yunnan, China (Table 1). The cultures were grown on Rye tomato agar [22]. The plant material potato 'S88' was provided by the Potato Disease Research Laboratory of Yunnan Agricultural University, Kunming, China. Potato 'S88' were grown for 45 days, and compound leaves from the top to the third leaf position were chosen for pathogen inoculation.

Phytophthora infestans inoculation on detached potato leaves

Leaves from potato 'S88' plants were removed and rinsed three times with sterile water to remove dust and other contaminants from the leaf surfaces. They were then placed with the upper surface facing up in a petri dish containing 0.8% water agar. Following the method of Wang et al. [23], a sporangial suspension at 8,000 sporangia/mL was prepared, and 25 µL of the suspension was deposited to either side of the leaf vein. Three leaves were inoculated per strain as replicates, and the procedure was conducted three times. The leaves were then turned over and incubated in an incubator at 19℃ for a cycle between light and darkness for 12-hour periods. Observations

were recorded three days after the incubaton began. The pathogenicity of *P. infestans* on potato leaves was determined by measuring the lesion area to total leaf area pixel ratio using Photoshop [24].

Biological characterization of *Phytophthora infestans* strains

Phytophthora infestans was cultured on rye tomato medium and incubated in the dark at 19 °C for 10 days. Following the method of Mu et al. [25], an 8 mm culture plug of *P. infestans* was cut using a cork borer, which was then placed in the center of the plate facing down. Each treatment had three replicates, and cultures were incubated at 19 °C in darkness for 4, 6, and 8 days. Colony diameter was measured perpendicularly, and mycelial growth was subsequently analyzed. After eight days of incubation, hyphae were scraped off and weighed using an analytical balance. The collected mycelia were then homogenized with water, and the number of sporangia was determined using a hemocytometer.

To assess the sensitivity analysis of *P. infestans* to metalaxyl (98%, RHAWN, Shanghai, China), the chemical was dissolved in dimethyl sulfoxide to create a 100 μg/mL stock solution. Rye tomato culture medium was prepared by adding metalaxyl at 5 μg/mL or 100 μg/mL. A culture plug (8 mm diameter) was placed in the center of the metalaxyl-amended plate. Each strain was treated with three replicates. The sensitivity of *P. infestans* to metalaxyl was evaluated by measuring colony diameter, mycelial weight and sporangial number after eight days of incubation in the dark at 19 °C.

Transcriptome analysis

Two *Phytophthora infestans* strains, HZ02 and DL04 with different virulence levels were inoculated onto detached potato leaves. Non-inoculated leaves were used as the control group (CK). After three days of inoculation, the leaves were collected, and flash-frozen in liquid nitrogen, and stored in a refrigerator at -80° C for later use. Total RNA was extracted from the leaves using the Total RNA Extractor Kit (Trizol, Sangon Biotech, Shanghai, China) according to the manufacturer instructions. The total RNA was quantified using the Qubit 2.0 RNA detection kit (Life Tech, Carlsbad, USA) to determine the amount of total RNA for library construction. The integrity and purity of total RNA were detected by 1% agarose gel electrophoresis and ultraviolet spectrophotometer (Inc SMA4000, Merinton Instrument, USA). RNA was considered of sufficient quality when the OD value A260/A280 was above 2.0.

The total RNA was subjected to mRNA isolation and fragmentation. The Hieff NGS™ Max Up Dual-mode mRNA Library Prep Kit (12301ES96, YEASEN, China) was used for reverse transcription to synthesize double-stranded cDNA. cDNA fragments were purified and size-selected using Hieff NGS™ DNA Selection Beads (12601ES56, YEASEN, China). The amplified library products underwent additional purification with the same bead-based system to ensure fragment size uniformity. The cDNA library clusters were generated using the cBot machine (Illumina, San Diego, CA, USA) [26].

Qualified samples were sequenced using the Illumina HiSeq 2500 platform (Shanghai Sangon, Shanghai, China). Raw reads were processed using FastQC (http://www.bioinformatics.babraham.ac.uk/projects/fastqc/) to remove adapters and low-quality sequences. Clean reads were then mapped to the reference genome downloaded from NCBI (http://ncbi.nlm.nih.gov/) using Hisat2 (https://ccb.jhu.edu/software/hisat2/index.shtml). Reads containing adapters, sequences with more than 10% unknown nucleotides, and those with an average quality score below Q20 were discarded [27].

All assembled unigenes were annotated using several databases, including NCBI NR (http://ncbi.nlm.nih.gov/), GO (http://www.geneontology.org), KEGG (http://www.kegg.jp), Pfam (http://pfam.xfam.org/), and KOG (https://www.ncbi.nlm.nih.gov/COG/). The sequencing data were analyzed to explore the relationship between the pathogenicity differences of various physiological races and genomic variations. This included Gene Ontology (GO) enrichment analysis and Kyoto Encyclopedia of Genes and Genomes (KEGG) pathway enrichment analysis to predict the potential functions of the identified genes. Gene expression levels were estimated as fragments per kilobase per transcript per million mapped reads (FPKM values). Principal component analysis (PCA) was performed on regularized log values of read counts. Differentially expressed genes (DEGs) between different treatments were restricted based on a false discovery rate ≤ 0.05 and an absolute value of $\log_2$Ratio ≥ 1 [27].

Validation of gene expression by quantitative real-time PCR (qRT-PCR)

Total RNA was extracted using the UNlQ-10 column Trizol Total RNA Extraction Kit. RNA degradation and contamination were assessed via 1.5% agarose gel electrophoresis. A total of 1500 ng of RNA was added to a nuclease-free PCR tube on ice. To the tube, 1 μL of Random Primer p(dN)6 (100 pmol), 1 μL of dNTP mix (0.5 mM final concentration), and RNase-free ddH_2O were added to bring the total volume to 14.5 μL. The mixture was gently shaken and briefly centrifuged for 3 to 5 s. The reaction was incubated at 65℃ for 5 min, followed by an ice bath for 2 min, and a brief centrifugation for 3 to 5 s. Following the ice bath, 4 uL of 5X RT buffer, 0.5 μL of Thermo Scientific RiboLock RNase Inhibitor (20 U), and 1 μL of Maxima Reverse Transcriptase (200 U) were

added to the reaction mixture. The reaction was gently mixed and centrifuged for 3 to 5 s. Reverse transcription reaction was then performed on a PCR instrument.

For fluorescence quantitative PCR, the cDNA sample was diluted 5-fold and used as a template, with the actin housekeeping gene as the target for amplification. The PCR primers were reactin-F2 (5' TGCCTGATG GACAAGTTATTACC 3') and actin-R2 (5' CCACTG AGCACAATGTTACCG 3'). The 10 mL PCR reaction mixture included 5 mL of 2X SybrGreen qPCR Master Mix, 0.2 mL of 10 mM primer F, 0.2 mL 10 mM R, 3.6 mL of ddH_2O, and 1.0 mL of cDNA. The thermal cycling conditions were as follows: 95 °C for 3 min, followed by 95 °C for 15 s, 60 °C for 30 s, for a total of 45 cycles. PCR products were analyzed using a Light Cycler480 II fluorescence quantitative PCR instrument (Roche, Rish-Rotkreuz, Switzerland). The relative expression of genes was calculated using the $2^{-\Delta\Delta CT}$ method. Three independent biological and technical replicates were conducted throughout the entire RNA extraction and sequencing workflow, ensuring methodological robustness.

Statistical analysis

Statistical analyses were performed using IBM SPSS Statistics version 25.0 software (SPSS Inc., Chicago, IL, USA) and GraphPad Prism 9.0 software (GraphPad Inc, San Diego USA). Prior to analyses, the normality of distribution and homogeneity of variance were assessed. Differences in means between treatments were evaluated using one-way ANOVA and Duncan's multiple range test ($P < 0.05$).

Results

Pathogenicity of *Phytophthora infestans* strains

The tested physiological races of *Phytophthora infestans* exhibited different levels of pathogenicity on detached potato leaves (Fig. 1) (Supplementary Table S1). Lesion areas ranged from 3.77 to 90.10%, indicating substantial pathogenic differences among the races. Strain HJG02, which harbors virulence factor 11(virulence factor reference Table 1), resulted in a lesion area of 60.43%, and was not significantly different from ML01-2019, which had lesion area of 56.46%. In contrast, LJ05 containing virulence factor 11 exhibited a lesion area of 24.18%, while DQ01 lacking virulence factor 11 showed a larger lesion area of 38.46%. DL04, deficient in virulence factor 7, displayed extensive lesions (76.26%), whereas HJG02 carrying virulence factor 7 developed markedly smaller lesions. MLS8802 demonstrated moderate lesions (48.49%), but HJG02 harboring virulence factor 1 produced significantly larger lesions. Notably, HZ02 lacking virulence factor 3 exhibited minimal lesions (12.66%), whereas DL04 with intact virulence factor 3 caused substantially larger lesions. Given the marked pathogenicity difference between HZ02 and DL04, further analysis will focus on biological characteristics and sensitivity to metalaxyl of these two strains with distinct virulence gene profiles.

Biological characterization of *Phytophthora infestans* strains HZ02 and DL04

There were significant differences in biological phenotypes between HZ02 and DL04 (Fig. 2). HZ02 exhibited shorter and sparser hyphae, while DL04 had longer and denser hyphae (Fig. 2a). Additionally, the mycelial growth of the strains diverged significantly over time, with DL04 consistently showing faster growth (Fig. 2b). The weight of mycelium from DL04 were significantly higher than that of HZ02 (Fig. 2c), and the number of sporangia per unit weight of mycelia from DL04 was slightly higher than that of HZ02, but the difference was not significant (Fig. 2d).

Sensitivity of *Phytophthora infestans* strains to metalaxyl

Significant difference in sensitivity to metalaxyl was observed between strains HZ02 and DL04, impacting mycelial growth, weight, and sporulation (Fig. 3). The growth of DL04 was significantly inhibited by metalaxyl compared to HZ02, which was more sensitive with an inhibition rate significantly higher than that of HZ02 (Fig. 3a, b).

Transcriptomic analysis

RNA-seq analysis was conducted on potato leaves infected by *Phytophthora infestans* DL04 and HZ02 to elucidate the causes of pathogenic differences between the two physiological races. Nine libraries (CK, DL04 and HZ02, three biological replicates for each treatment) were generated, yielding approximately 75.13 Gb clean nucleotide sequences, with average Q20 and Q30 values of 97.38% and 93.53%, respectively, and an average GC content of 48.00%. Clean data matching to the reference genome showed that alignment rates between 92.96% and 94.16% across the nine samples (Supplementary Table S2), indicating high-quality sequencing suitable for further analysis.

The transcriptome profiles of *P. infestans* changed after *P. infestans* DL04 and HZ02 strains infected potato leaves. Functional annotation was performed across multiple databases including NR, GO, KEGG, Pfam, KOG, and SwissProt databases, with 20,036, 17,312, 8636, 10,891, 13,021, and 10,593 annotated uniqueness respectively (Supplementary Table S3). GO enrichment analysis categorized the differentially expressed genes (DEGs) (Supplementary Figure S1), revealing that 17 terms related to biological processes were dominant, particularly those associated with metabolic process, cellular process, and biological regulation. The cellular component category

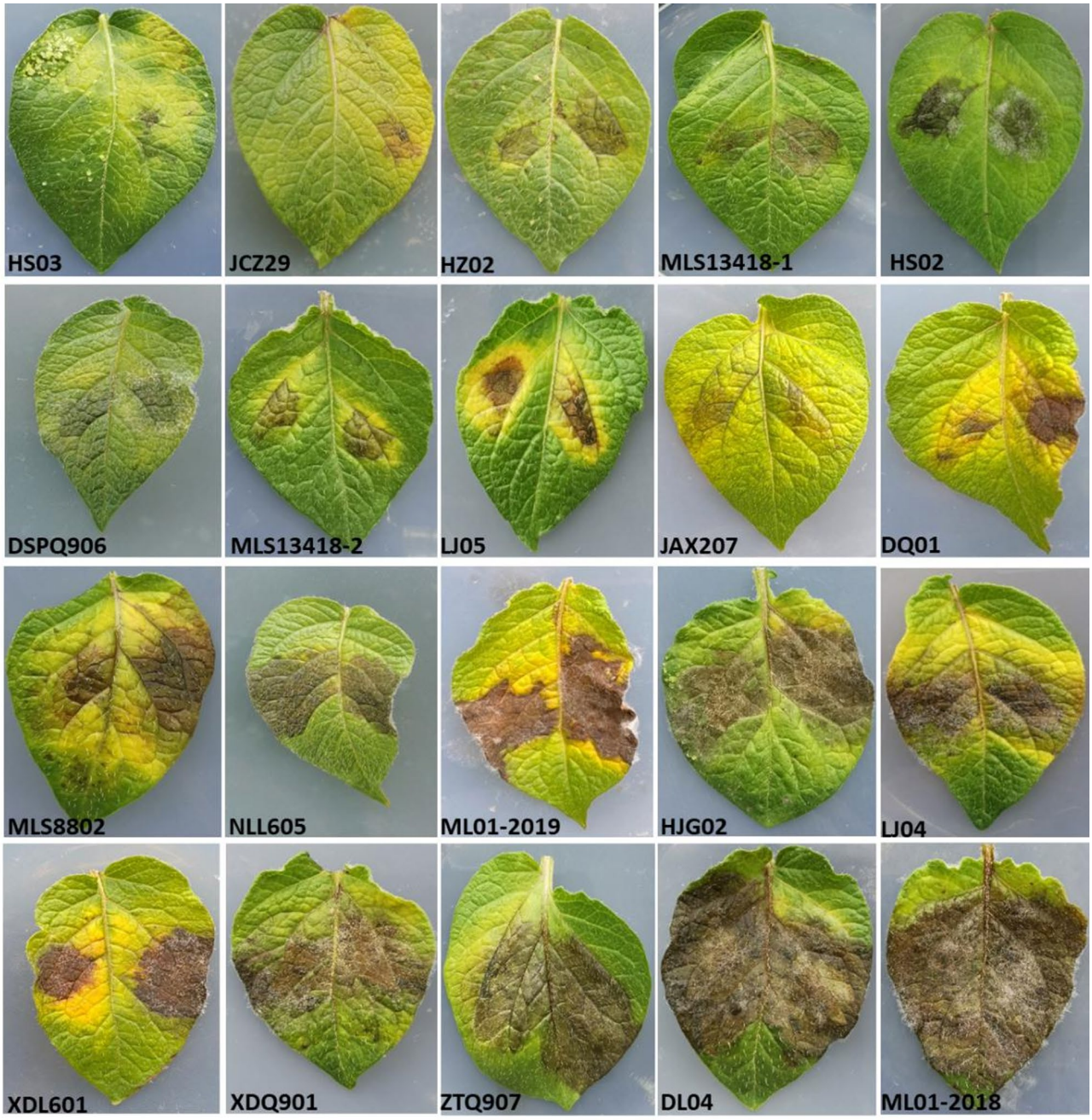

Fig. 1 Pathogenicity assay of *Phytophthora infestans* strains on potato detached leaves observed three days after inoculation. Each image displays representative lesions derived from three biological replicates

contained 12 terms, primarily involving the cell, cell parts, and organelles. Additionally, two terms in the molecular function category, binding and catalytic activities, were enriched.

PCA showed that DL04 and HZ02 inoculations were significantly separated from the control group. PC1 and PC2 accounted for 48.79% and 20.03% of the variation, respectively, indicating substantial gene expression differences between the treatments (Fig. 4a). Differential expression analysis using DESeq and based on FPKM identified 1,482, 9,525, and 1,851 DEGs for the HZ vs. CK, DL vs. CK and DL vs. HZ comparisons, respectively. Interestingly, the number of genes that were significantly upregulated and downregulated differed across each comparison group (Fig. 4b, Supplementary Figure S2), highlighting a significant shift in gene expression post-inoculation with DL04, which contains virulence factor 3.

KEGG pathway enrichment analysis for the DL vs. HZ comparison identified 30 significantly enriched pathways ($P < 0.05$), including carbon metabolism, biosynthesis of

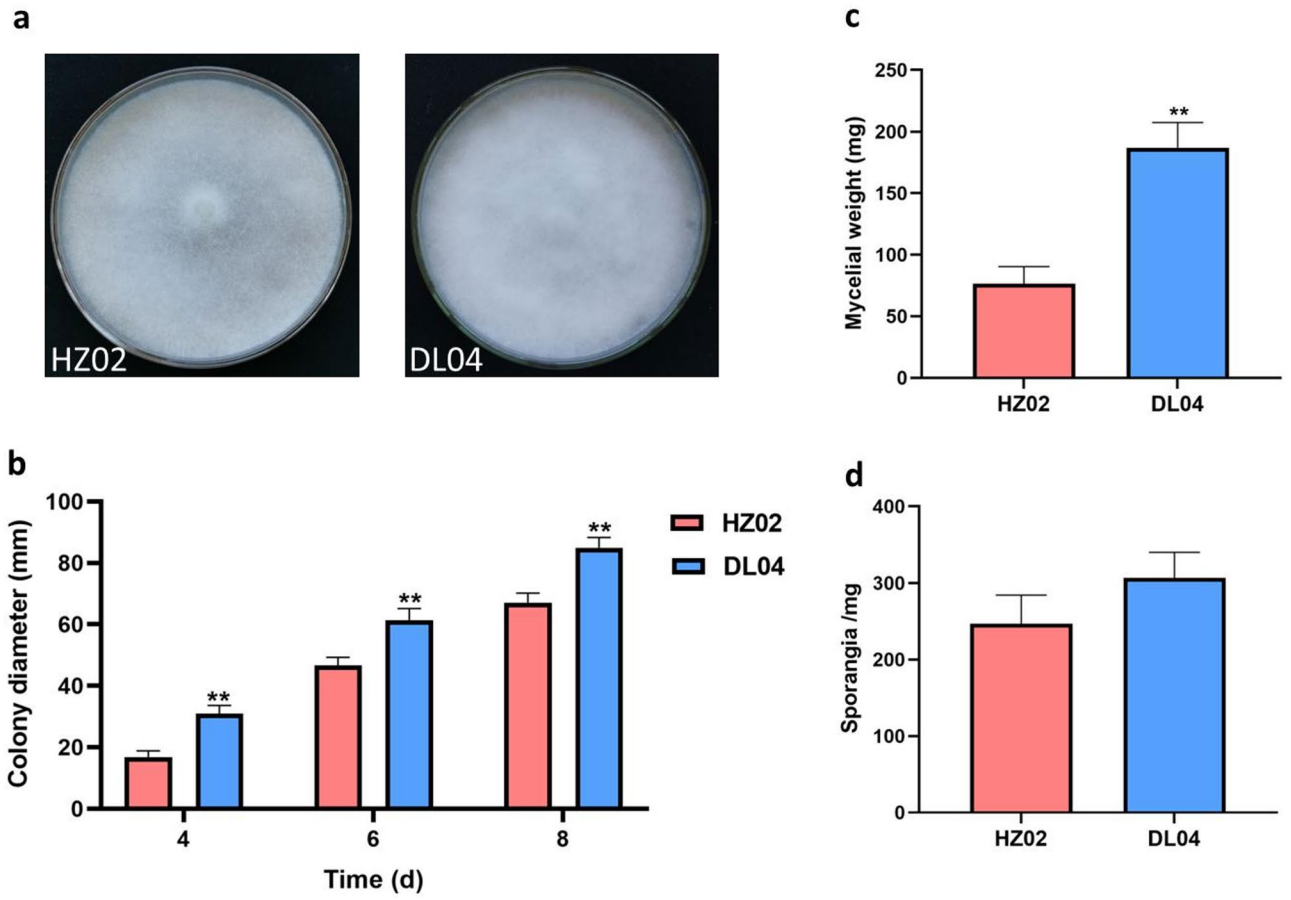

Fig. 2 Comparisons of *Phytophthora infestans* strains HZ02 and DL04: (**a**) culture morphology after 8 days of incubation, (**b**) mycelial growth over 4, 6, and 8 days, (**c**) mycelial weight, and (**d**) sporangia count per unit of mycelial weight. Error bars represent standard deviations. Asterisks (**) indicate a significant difference between the strains ($P < 0.01$)

amino acids, glycolysis/gluconeogenesis, peroxisome, fatty acid metabolism, fatty acid degradation, valine, leucine and isoleucine degradation, glyoxylate and dicarboxylate metabolism, and tyrosine metabolism (Fig. 4c). In the carbon metabolic pathway, 38 genes were upregulated and two downregulated genes; and the glycolysis/gluconeogenesis pathway had 19 upregulated and one downregulated genes (Fig. 4d). These pathways, relating to sugar and acid metabolism and degradation, suggest that DL04 induces significant metabolic changes upon infecting potato leaves.

After inoculation with *P. infestans* DL04, a strain with strong pathogenicity that carries virulence factor 3, the gene expression significantly changed in the infected potato leaves. This variation in gene expression was linked to difference in the pathogenicity of the leaves. Further analysis showed a significant upregulation of genes in key pathways, including carbon metabolism, biosynthesis of amino acids, and glycolysis/gluconeogenesis, with a total of 82 genes significantly upregulated across these pathways (Fig. 5, Supplementary Table S5). In the carbon metabolism pathway, genes with the higher fold increase included threonine dehydratase (*TdcB*), formate dehydrogenase (*FDH*), Aminomethyltransferase (*AMT*), isocitrate dehydrogenase (*IDH*), acyl-CoA dehydrogenase (*CADD*), and acetyl-coenzyme A synthetase (*Acetyl-CoA*).

In the biosynthesis of amino acids pathway, notable upregulations were observed in genes such as threonine dehydratase catabolic (*TdcB*), acetylornithine aminotransferase (*argD*), dihydroxy-acid dehydratase (*IIvD*), aspartate aminotransferase (*AST*), chorismate synthase, tyrosine aminotransferase (*TAT*), aldehyde dehydrogenase (*ALDH*), and isocitrate dehydrogenase (*IDH*). In the glycolysis/gluconeogenesis pathway, significant upregulations included genes such as aldehyde dehydrogenase (*ALDH*), aldose 1-epimerase, and acetyl-coenzyme A synthetase (*Acetyl-CoA*).

Additionally, pathway enrichment analysis identified several cell-wall-hydrolysis genes that were significantly upregulated (Table S6), including pectinesterase (*PE*), glycoside hydrolase (*GH*), polygalacturonase (*PG*), cell 5 A endo-1.4-betaglucanase (*EG*), aldehyde dehydrogenase (*ALDH*), fructokinase (*FRK*), glucose-6-phosphate

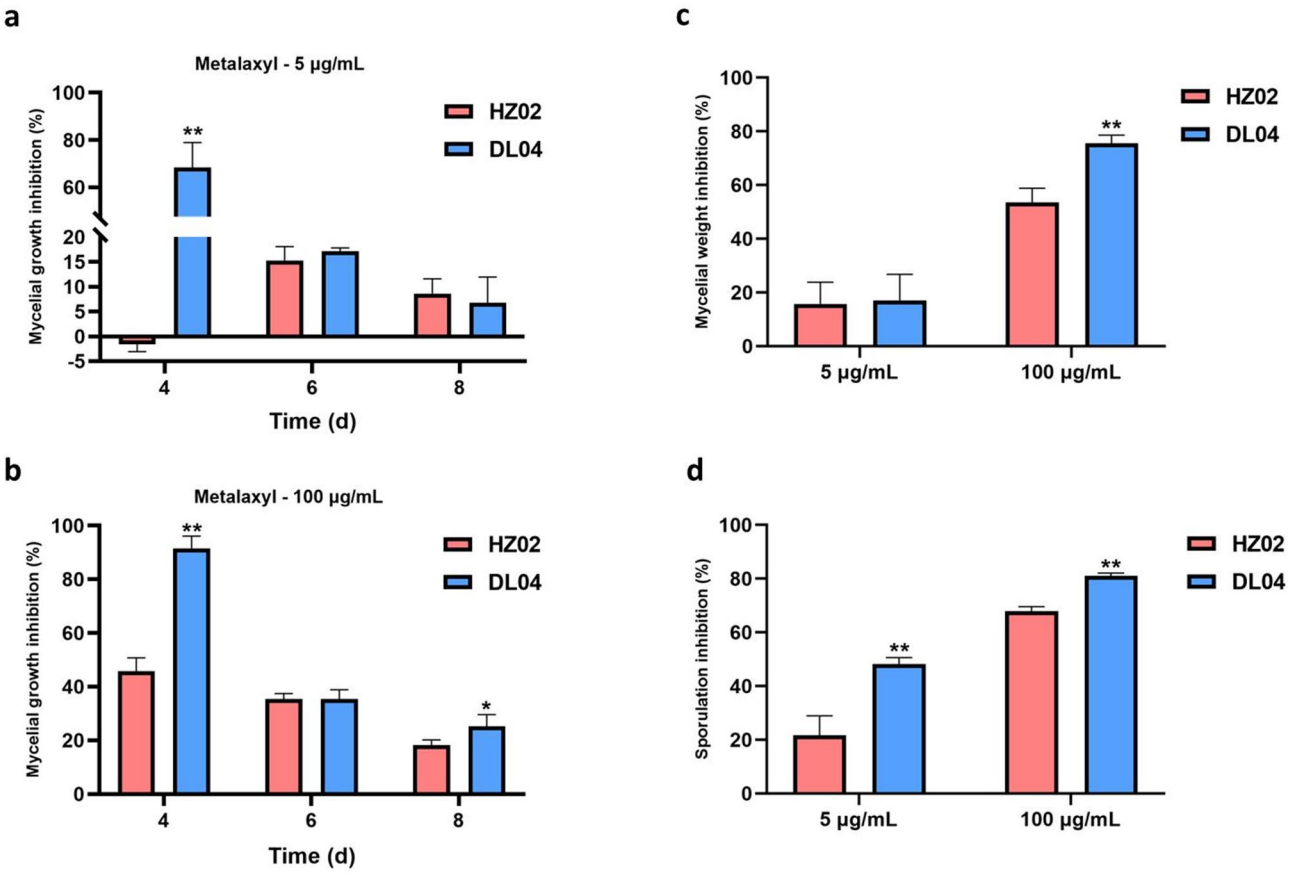

Fig. 3 Comparisons of *Phytophthora infestans* strains HZ02 and DL04 in response to metalaxyl: (**a**, **b**) mycelial growth, (**c**) mycelial weight, and (**d**) sporulation. Error bars represent standard deviations. Significant differences between the strains were indicated by asterisks ** ($P < 0.01$) or * ($P < 0.05$)

isomerase (*GPI*), cellulose synthase (*CESA*), chitinase (*CHT*), and cysteine protease (*CPs*). Compared to the control, the pectinesterase genes *PEs* (PITG_06560 and PITG_08912) were upregulated 18.17- and 17.44-fold, respectively. The polygalacturonase gene *PG* (PITG_19624) exhibited a 17.19-fold increase, and glycoside hydrolase genes *GH* (PITG_17546 and PITG_04135) were upregulated 17.15- and 18.24-fold. The results showed that these genes involved in cell wall degradation were significantly expressed during the infestation of *P. infestans*.

From the pool of candidate DEGs, genes encoding PE, PG, GH, ALDH, and EG were selected for qRT-PCR analysis to validate the transcriptomic data. The relative expression of *PITG-01029* encoding PE and *PITG03136* encoding GH was significantly upregulated (Fig. 6b, e). Compared with strain HZ02, the relative expression of DEGs encoding PG, ALDH and EG was upregulated, but the increase was not statistically significant (Fig. 6d, f, g). These results corroborated the expression trends observed in the transcriptome sequencing, affirming the reliability of the sequencing results.

Discussion

Metabolic pathways play a key role in pathogen infection, affecting energy acquisition and metabolic processes [28, 29]. Our analysis revealed that carbon metabolism, biosynthesis of amino acids, and glycolysis/gluconeogenesis pathways were significantly enriched in potato leaves following infection by *Phytophthora infestans* strain DL04, suggesting their potential involvement in pathogenic processes. Emerging evidence indicates that metabolic pathways play regulatory roles in modulating the virulence mechanisms of phytopathogens during host colonization. Similar studies have identified carbon metabolism as a significantly enriched pathway in *Xanthomonas oryzae*, demonstrating that carbon source acquisition critically facilitates pathogen-host interaction establishment and proliferative growth [30]. Carbon storage is also vital for oomycetes, particularly in oospores. Unlike most fungal spores, oospores possess metabolic activity. These reserves are necessary to support germ tube formation and host penetration [31]. Through transcriptomic profiling revealed that distinct enrichment of glycolysis/gluconeogenesis pathways in KEGG functional annotation when comparing differential gene expression between

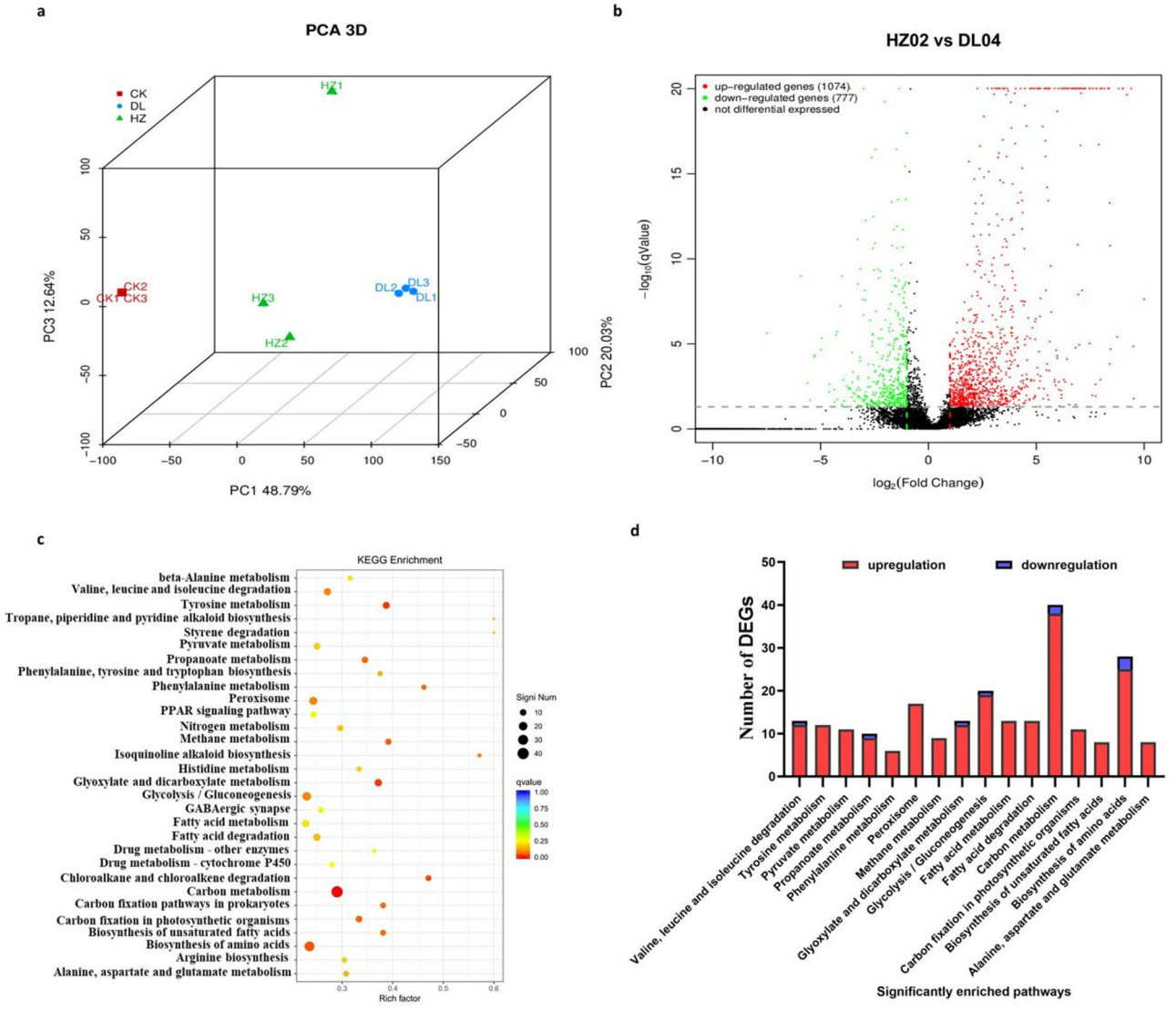

Fig. 4 Transcriptomic analysis of potato leaves inoculated with different physiological races of *Phytophthora infestans*. (**a**) Principal component analysis (PCA) showing the distribution of transcriptomic data points. (**b**) Volcano plot of gene expression variance of *P. infestans* strains HZ02 and DL04. Red indicates significant upregulation, green indicates significant downregulation, and black represents gene expressions with no significant differences. The horizontal axis displays log2 fold change in gene expression, while the vertical axis represents the q-value. (**c**) Kyoto Encyclopedia of Genes and Genomes (KEGG) pathway enrichment analysis for DL and HZ inoculations. The vertical axis indicates pathways, and the horizontal axis indicates the enrichment factor (Ratio of differentially expressed genes (DEGs) to total annotated genes in each KEGG pathway) corresponding for each pathway. Dotted points represent *P*-value significance, with darker red indicating higher significance. The size of each dot represents the number of differentially expressed metabolites. (**d**) Differential gene expression in enrichment pathways comparing DL04 and HZ02 inoculations. Red bars indicate upregulated gene expression and blue bars show downregulated gene expression

pathogenic variants *Sporisorium scitamineum* Ss16 and Ss47 [32]. The bE/bW heterodimeric transcription factor encoded by the b locus modulates sexual mating and/or filamentous growth in *S. scitamineum* through coordinated regulation of sugar metabolism and Hog1-mediated oxidative responses [33]. Glycolysis is recognized as a central metabolic pathway essential for pathogenesis in several pathogens [34], including *Candida albicans*, where it supports surface adhesion, virulence, and are responsiveness under specific environmental conditions [35]. These related pathways are indirectly involved in the pathogenic process. These studies reported similar results to the present study, suggesting that carbon metabolism and glycolysis/glycolysis pathways are associated with the infestation process of pathogenic. We hypothesize that during late blight pathogenesis, *P. infestans* may assimilate carbon sources to fuel carbohydrate metabolism and related pathways, thereby supplying carbon skeletons for biosynthesis of amino acids while potentially mediating direct or indirect signaling cascades critical to virulence.

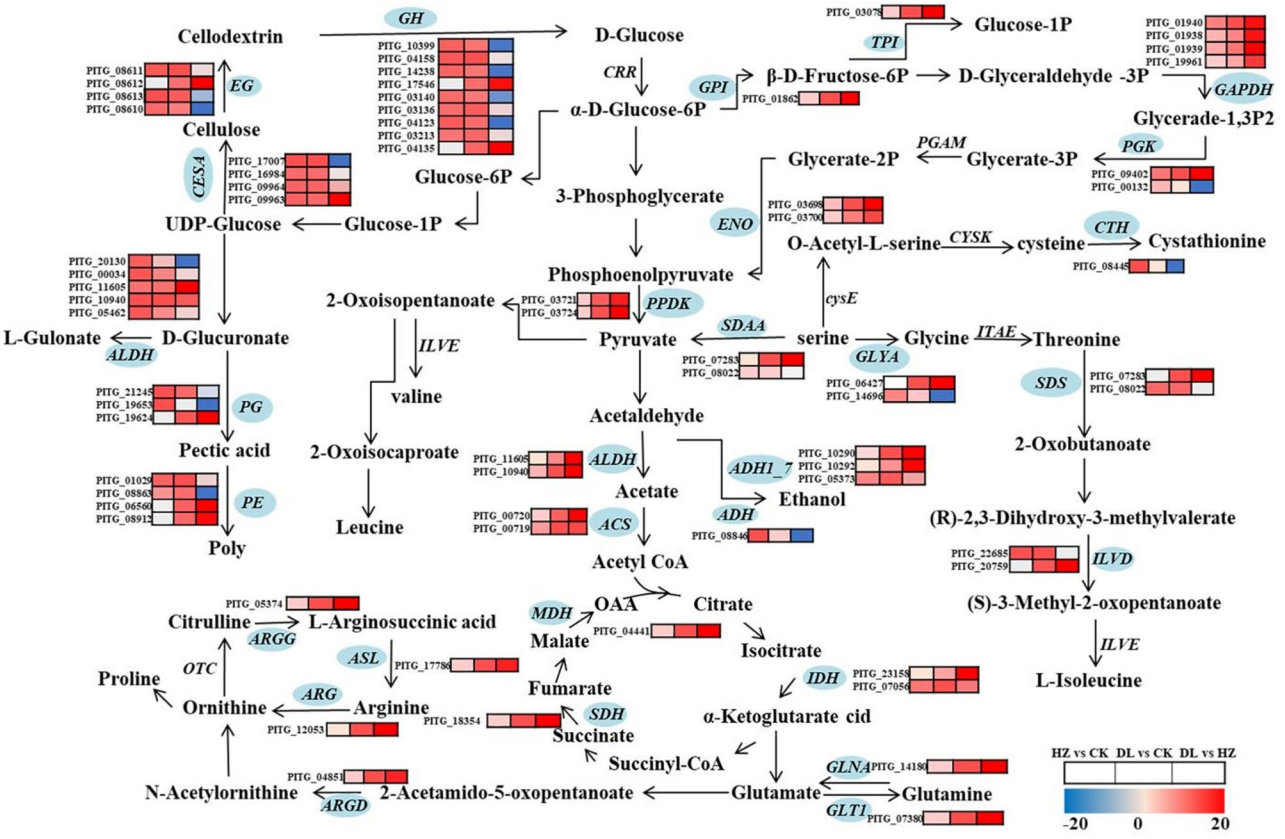

Fig. 5 Schematic diagram of patterns related to significantly enriched pathways in potato infected by *Phytophthora infestans* strains DL04 and HZ02. The blue ellipse represents genes that are significantly enriched in DL04 and HZ02 inoculations. The heatmap shows differential gene expression, with each square representing comparisons: HZ02 vs. CK (non-inoculated control), DL04 vs. CK, and DL04 vs. HZ02. The expression levels of annotated genes are represented in the heatmap, with a color scale ranging from blue (-20) to red (20), indicating the extent of gene expression changes

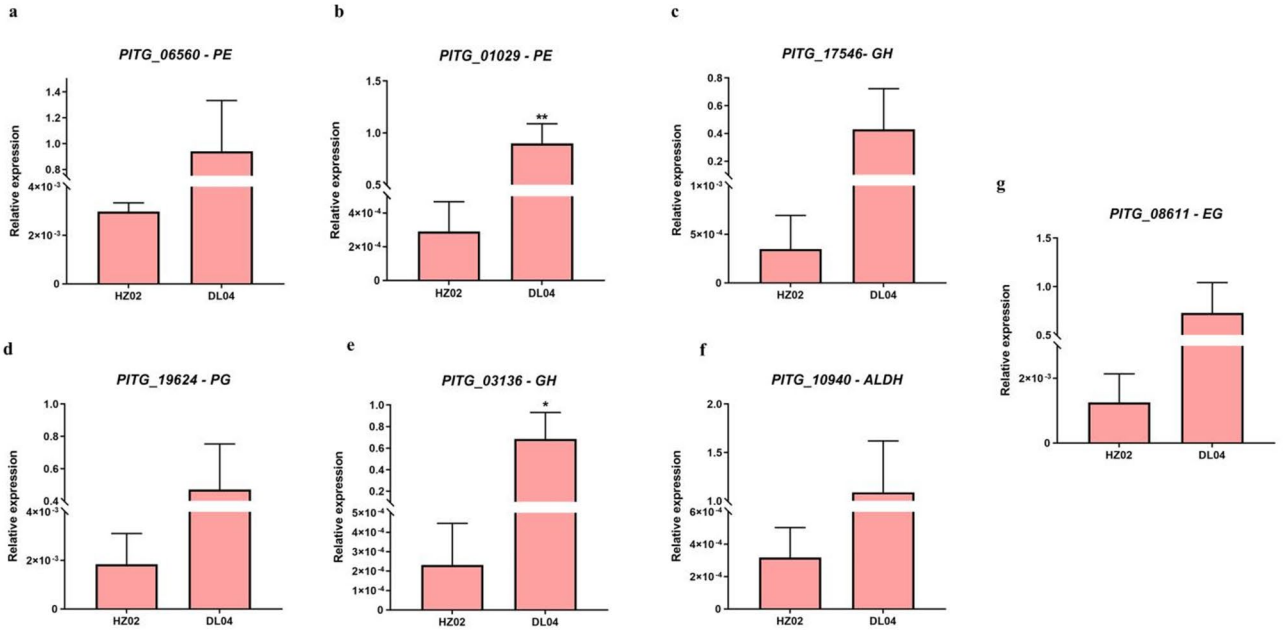

Fig. 6 Relative gene expression in potato leaves treated with *Phytophthora infestans* strains DL04 and HZ02, as verified by quantitative polymerase chain reaction (qPCR). Significant differences are indicated by asterisks ** ($P < 0.01$) and * ($P < 0.05$)

Subsequently, the metabolic pathway will be further analyzed and its main role in the pathogenesis will be verified.

The plant cell wall serves as the first line of defense against pathogen infection [36]. To overcome this obstacle, plant pathogens produce various cell wall-degrading enzymes during the pathogenic process. Plant pathogens deploy extracellular hydrolases such as endopolygalacturonase (endo-PG) and pectin methylesterase (PME), which are essential for pathogen colonization [37]. In this study, infection of potato leaves by *P. infestans* DL04, which harbors virulence factor 3, led to the significant upregulation of genes encoding cell wall-degrading enzymes. These included pectin methylesterase (PE), endopolygalacturonase (PG), glycoside hydrolase (GH), glucanase (EG), and cellulose synthase (CESA). These genes play a key role in plant growth and development, and it is speculated that the pathogenic differences observed may be due to the differential expression of genes involved in cell wall degradation. Several studies have shown that cell wall degrading enzymes play a key role in pathogenicity, for example, the pectin methylesterase Pcpme6 from *Phytophthora capsici* has been shown to exhibit strong virulence and diverse transcriptional responses when infecting different hosts [38]. Plant pathogens can degrade plant cell walls by secreting glycoside hydrolase XEG1 to promote infection in the early stage of infection [39]. PG penetrates plant cell walls and accelerates host invasion [40]. Expression of a gene encoding a pectin hydrolase was found to be associated with pathogenicity of *Fusarium solani*, and pathogenicity was reduced only when expression was suppressed [41]. Similarly, mutations in the endogenous polygalacturonase gene of *Alternaria alternata* infecting citrus fruits weakened the fungus' pathogenicity [42]. These findings indicate that cell wall-degrading enzymes are crucial pathogenic factors in the process of pathogen infection. Therefore, the difference in pathogenicity among different physiological races of *P. infestans* may be partially due to the different expressions of genes encoding cell wall-degrading enzymes. Previously, we have identified pectinesterase as a key factor responsible for the virulence differences, as pectinesterase activity and its gene expression are positively correlated with the pathogenicity of *P. infestans* [43]. In addition to pectinesterase, other cell wall-degrading genes should be investigated in subsequent studies. Reportedly, the effector proteins PcPL1, PcPL15, PcPL16, and PcPL20 of *P. capsici* can induce plant cell death [44].

With the ongoing evolution of *P. infestans* physiological races, previously effective resistance genes have lost their functionality [45]. Effectors play a crucial role in the interaction between pathogen and hosts, directly affecting the invasion, expansion, and disease occurrence [46]. To successfully invade and reproduce in host plants, avirulence genes (*Avr*) in *P. infestans* can mutate to evade recognition by these resistance genes [47, 48]. For example, the host R3 haplotype, corresponding to virulence factor 3 contained two major resistance gene clusters *R3a* and *R3b*, which have been confirmed with their corresponding avirulence genes, *Avr3a* [49] and *Avr3b* in *P. infestans* [50]. Interestingly, the avirulence gene *Avr3a*, which corresponds to the host major resistance gene *R3*, was found in the sequencing results, and the expression level was significantly up-regulated after DL04 infection, with an upregulated 21.59-fold. However, *Avr3b* was not found in the data, indicating that *Avr3a* may also be involved in the pathogenesis (Supplementary Table S4). It is speculated that the difference in virulence factors may not only be related to the pathogenicity of *P. infestans*, but also to the participation of avirulence genes in plant-pathogen interactions. *Avr3a* is known to trigger plant immune responses and manipulate defense pathways [51]. Avr3a-like effectors, widely conserved in *Phytophthora* species, orchestrate multifaceted immune suppression in host plants. These effectors stabilize *Arabidopsis* CAD7 subfamily member AtCAD7, directly impairing PAMP-triggered immunity (PTI) by reducing callose deposition, ROS bursts, and *WRKY33* expression [52]. Additionally, AVR3a stabilizes the host E3 ligase *CMPG1* to block programmed cell death (PCD) during biotrophic growth, ensuring pathogen survival [53]. Beyond PTI/PCD suppression, AVR3a disrupts immune receptor endocytosis by targeting a membrane-trafficking complex, thereby inhibiting BAK1/SERK3-mediated immunity through distinct pathways, exemplifying its multifunctional virulence [54]. In addition, dsRNA targeting *Avr3a* effectively inhibited *P. infestans* infection, enabling plants to obtain balanced immunity and enhanced defense [55]. Specifically, *Avr3a* can inhibit host defense signals and enhance pathogen infection by regulating the interaction of immune factors in host plants. Although the study of the effector Avr3a has shed light on its role in pathogenicity and its mechanisms, the full scope of interactions between avirulence gene and host proteins are still unclear. Subsequent studies will focus on elucidating the molecular mechanism of the interaction between the Avr3a effector and the host. Mutations in *Avr3a* may lead to the breakdown of R3a-mediated resistance, thus necessitating continuous monitoring of the pathogen population's genetic structure. The transcriptome markers obtained in this study can be utilized to monitor Avr3a variants for predicting resistance efficacy and formulating rotation strategies for potato cultivars carrying different R genes. Assisted rapid screening enables efficient identification of potato germplasm resources harboring the *R3a* resistance gene.

Conclusion

Phytophthora infestans DL04 demonstrated strong pathogenicity, alongside fast growth, substantial mycelial production, and high sensitivity to metalaxyl. The pathogenicity of DL04 was closely linked to the expression of virulence factor 3, which activated key metabolic pathways related to the pathogenesis, including carbon metabolism, glycolysis, and biosynthesis of amino acids. This resulted in the upregulation of genes involved in cell hydrolysis, significantly contributing to its enhanced ability to infect and damage potato leaves. The study also highlighted the crucial role of cell wall-degrading enzymes, such as pectinesterase, polygalacturonase, and glycoside hydrolases, in the infection process. Furthermore, the upregulation of the avirulence gene *Avr3a* suggests that the interaction between virulence and avirulence factors plays an important role in the pathogen's ability to evade host defense responses and facilitate infection. Transcriptome markers enable *Avr3a* variant tracking to optimize R gene-based cultivar rotation and predict resistance durability. Transcriptomics reveals *P. infestans* pathogenesis mechanisms, underscoring the need to target Avr3a effectors and cell wall-degrading enzymes for durable resistance breeding. These findings are of great significance for effector recognition and modulating cell wall-degrading enzymes activity to enhance disease management.

Supplementary Information

The online version contains supplementary material available at https://doi.org/10.1186/s12870-025-06736-y.

Supplementary Material 1: **Table S1**. Lesion area of potato leaves infected by different ***Phytophthora infestans*** strains.

Supplementary Material 2: **Table S2**. Sequencing output statistics table.

Supplementary Material 3: **Table S3**. Unigenes corresponding to single genes annotated in the database.

Supplementary Material 4: **Table S4**. The expression of Avr3a gene in three treatments.

Supplementary Material 5: **Table S5**. Significantly up- and down-regulated genes in the three pathways after inoculation of potato leaves with ***Phytophthora infestans*** DL04 strain.

Supplementary Material 6: **Table S6**. Comparison of expression levels of hydrolysis-related genes in different treatments.

Supplementary Material 7: **Figure S1**. GO functional classification of leaves infected by ***Phytophthora infestans***.

Supplementary Material 8: **Figure S2**. Volcano plot of differentially expressed genes.

Acknowledgements
Not applicable.

Author contributions
Y.L.Y and X.L designed the study, L.M.D completed the data analysis and wrote the manuscript, Y.L.Y, X.L, and J.J.H improved and revised the writings. J.W.F, J.Z, J.D, and G.H.X facilitated data collection. K.Y.Z, Y.J.X, W.P.W, and S.H.Z Completed the Determination of data. C.J.L and M.C completed the verification of the test. All authors discussed the results and contributed to the final manuscript.

Funding
This work was supported by the National Key Research and Development Program of China (2024YFD1401200), the Modern Agricultural Potato Industry Technology System in Yunnan Province (2024KJTX-04), the Major Science and Technology Projects in Yunnan Province (202402AE090017).

Data availability
Sequence data that support the findings of this study have been deposited in the NCBI (National Center for Biotechnology Information) SRA repository with the primary accession code PRJWB13140.

Declarations

Ethics approval and consent to participate
Not applicable.
All the plant materials in this paper comply with relevant institutional, national, and international guidelines and legislation.

Consent for publication
Not applicable.

Competing interests
The authors declare no competing interests.

Received: 27 January 2025 / Accepted: 16 May 2025
Published online: 28 May 2025

References

1. Chen XK, Wang WB, Cai PP, Wang ZW, Li TT, Du Y. The role of the MAP kinase-kinase protein *STMKK1* in potato immunity to different pathogens. Hortic Res. 2021;8(1):117.
2. Black W, Mastenbrock C, Mills WR, Peterson LC. A proposal for an international nomenclature of races of *Phytophthora infestans* and of genes controlling immunity in Solanum demissum derivaties. Enphytica. 1953;2(3):173–9.
3. Zheng KK, Lu J, Li J, Yu Y, Zhang J, He ZW, et al. Efficiency of Chitosan application against *Phytophthora infestans* and the activation of defence mechanisms in potato. Int J Biol Macromol. 2021;182:1670–80.
4. Wang XD, Zheng KK, Cheng WY, Li J, Liang XX, Shen J, et al. Field application of star polymer-delivered Chitosan to amplify plant defense against potato late blight. Chem Eng J. 2021;417:129327.
5. Fry WE, Birch PRJ, Judelson HS, Grünwald NJ, Danies G, Everts KL, et al. Five reasons to consider *Phytophthora infestans* a reemerging pathogen. Phytopathology. 2015;105(7):966–81.
6. Michalska AM, Sobkowiak S, Flis B, Zimnoch-Guzowska E. Virulence and aggressiveness of *Phytophthora infestans* isolates collected in Poland from potato and tomato plants identified no strong specificity. Eur J Plant Pathol. 2016;144:325–36.
7. Cohen Y. Populations of *Phytophthora infestans* in Lsrael underwent three major genetic changes during 1983 to 2000. Phytopathology. 2002;92(3):300–7.
8. Runno-Paurson E, Fry WE, Myers KL, Koppel M, Mänd M. Characterisation of *Phytophthora infestans* isolates collected from potato in Estoniaduring 2002–2003. Eur J Plant Pathol. 2009;124(4):565–75.
9. Runno-Paurson E, Ronis A, Hansen M, Aav A, Williams IH. Lithuanian populations of *Phytophthora infestans* revealed a high phenotypic diversity. J Plant Dis Protect. 2015;122(2):57–65.
10. Aav A, Skrabule I, Bimšteine G, Kaart T, Williams IH, Runno-Paurson E. The structure of mating type, Metalaxl resistance and virulence of *Phytophthora infestans* isolates collected from Latvia. Zemdirbyste. 2015;102(3):335–42.
11. Shu Y. A preliminary study on the population genetic structure of *Phytophthora infestans* isolates collected from Anhui, Fujian and Hunan provinces in China. Nanjing Agricultural University; 2015. [in Chinese]

12. Chen Q, Li Y, Zhang M, Peng HX, Xi YD, Xu CY, et al. Genetic variation of *Phytophthora infestans* detected by SSRs in Sichuan Province. Southwest China Journal of Agricultural Sciences. 2010;23:91–7. [in Chinese]
13. Sun HH, Wang J. Study on the composition and distribution of physiological races of *Phytophthora infestans* in Qinghai. Mod Agricultural Sci Technol. 2008;11:111–2.
14. Chen XJ, Hao XR, Akhberdi O, Zhu XD. Genomic and transcriptomic survey provides insights into molecular basis of pathogenicity of the sunflower pathogen *Phoma Macdonaldii*. J Fungi (Basel). 2023;9(5):520.
15. Wrzesińska-Krupa B, Szmatoła T, Praczyk T, Obrępalska-Stęplowska A. Transcriptome analysis indicates the involvement of herbicide-responsive and plant–pathogen interaction pathways in the development of resistance to ACCase inhibitors in Apera spica-venti. Pest Manag Sci. 2023;79(5):1944–62.
16. Xie YF, Niu XF, Jiang XF, Liu SS, Wang ML. Comparison of alternative splicing of Brassica napus Dwarf mutant and its tall-stalked parents by using RNA-seq. J Application Environ Biology. 2018;24(1):81–8.
17. Tian L, Shi SH, Nasir F, Chang CL, Li WQ, Tran LP, et al. Comparative analysis of the root transcriptomes of cultivated and wild rice varieties in response to *Magnaporthe oryzae* infection revealed both common and species-specific pathogen responses. Rice. 2018;11(1):26.
18. Jacobs JM, Babujee L, Meng F, Milling A, Allen C. The *in planta* transcriptome of *Ralstonia solanacearum*: conserved physiological and virulence strategies during bacterial wilt of tomato. mBio. 2012;3(4):e00114–12.
19. Ah-Fong AMV, Kim KS, Judelson HS. RNA-seq of life stages of the oomycete *Phytophthora infestans* reveals dynamic changes in metabolic, signal transduction, and pathogenesis genes and a major role for calcium signaling in development. BMC Genomics. 2017;18(1):198.
20. Roquigny R, Novinscak A, Arseneault T, Joly DL, Filion M. Transcriptome alteration in *Phytophthora infestans* in response to phenazine-1-carboxylic acid production by *Pseudomonas fluorescens* strain LBUM223. BMC Genomics. 2018;19(1):474.
21. Gao L, Bradeen JM. Contrasting potato foliage and tuber defense mechanisms against the late blight pathogen *Phytophthora infestans*. PLoS ONE. 2016;11(7):e0159969.
22. Qian HJ, Liu X, Guo L, Zhang Z, Li GJ, Yang L, et al. Sensitivity determination of *Phytophthora infestans* to Metalaxyl in spring potato planting area of Yunnan Province. Acta Agriculturae Boreali-occidentalis Sinica. 2021;3(7):1083–8. [in Chinese]
23. Wang XG, Liu X, Zhang Z, Huang X, Deng LM, Xu GH, et al. Effects of VdAL on occurrence of potato late blight. Acta Agric Jiangxi. 2022;34(10):101–7. [in Chinese]
24. Cui HW, Yang YL, Li JT, Luo WF, Miao AM, Hu ZX, et al. A faster method for measuring relative lesion area on leaves based on software photoshop. J Anhui Agri Sci. 2009;37(22):10760–2. [in Chinese].
25. Mu QH, Lin R, Zhu N, Bai W. Isolation, identification and characteristic analysis of *Phytophthora infestans* on potatoes in Ulanqab, inner mongolia. Journal of Inner Mongolia Agricultural University. 2023;44(1):7–12. [in Chinese]
26. Lu XY, Li JQ, Yang JH, Liu XN, Ma J. De Novo transcriptome of the desert beetle *Microdera punctipennis* (Coleoptera: Tenebrionidae) using illumina RNA-seq technology. Mol Biol Rep. 2014;41(11):7293–303.
27. Deng LM, Luo LF, Li Y, Wang LT, Zhang JX, Zi BX, et al. Autotoxic ginsenoside stress induces changes in root exudates to recruit the beneficial Burkholderia strain B36 as revealed by transcriptomic and metabolomic approaches[J]. J Agric Food Chem. 2023;71(11):4536–49.
28. Neil H, Hnatova M, Wesolowski-Louvel M, Rycovska A, Lemaire M. Sck1 activator coordinates glucose transport and Glycolysis and is controlled by Rag8 casein kinase I in *Kluyveromyces lactis*. Mol Microbiol. 2007;63(5):1537–48.
29. Cairey-Remonnay A, Deffaud J, Wésolowski-Louvel M, Lemaire M, Soulard A. Glycolysis controls plasma membrane glucose sensors to promote glucose signaling in yeasts. Mol Cell Biol. 2015;35(4):747–57.
30. Guo W, Cai LL, Zou HS, Ma WX, Liu XL, Zou LF, et al. Ketoglutarate transport protein KgtP is secreted through the type III secretion system and contributes to virulence in *Xanthomonas oryzae* Pv. Oryzae. Appl Environ Microbiol. 2012;78:5672–81.
31. Ball S, Colleoni C, Cenci U, Raj JN, Tirtiaux C. The evolution of glycogen and starch metabolism in eukaryotes gives molecular clues to understand the establishment of plastid endosymbiosis. J Exp Bot. 2011;62(6):1775–801.
32. Wu J, Li HZ, Deng QQ, Chen JW, Shen WK. Sequencing of transcriptome of sporisorium Scitamineum with different pathogenicity. Journal of Huazhong Agricultural University. 2020;39(03):54–9. [in Chinese].
33. Yan MX, Dai WJ, Cai EP, Deng YZ, Chang CQ, Jiang ZD, et al. Transcriptome analysis of *Sporisorium Scitamineum* reveals critical environmental signals for fungal sexual mating and filamentous growth. BMC Genomics. 2016;17:1–11.
34. Chi PI, Huang WR, Chiu HC, Li JY, Nielsen BL, Liu HJ. Avian reovirus σA-modulated suppression of lactate dehydrogenase and upregulation of Glutaminolysis and the mTOC1/eIF4E/HIF-1α pathway to enhance Glycolysis and the TCA cycle for virus replication. Cell Microbiol. 2018;20(12):e12946.
35. Kumar R, Maulik M, Pathirana RU, Cullen PJ, Edgerton M. Sho1p connects Glycolysis to Ras1-cAMP signaling and is required for microcolony formation in *Candida albicans*. mSphere. 2020;5(4):e00366–20.
36. Zhao ZT, Liu HQ, Wang CF, Xu JR. Comparative analysis of fungal genomes reveals different plant cell wall degrading capacity in fungi. BMC Genomics. 2013;14(1):274.
37. Ma ZC, Zhu L, Song TQ, Wang Y, Zhang Q, Xia YQ, et al. A paralogous decoy protects *Phytophthora Sojae* apoplastic effector PsXEG1 from a host inhibitor. Science. 2017;355(6326):710–4.
38. Feng BZ, Li PQ, Wang HM, Zhang XG. Functional analysis of *Pcpme6* from oomycete plant pathogen *Phytophthora capsici*. Microb Pathog. 2010;49(1–2):23–31.
39. De Lorenzo G, Ferrari S. Polygalacturonase-inhibiting proteins in defense against phytopathogenic fungi. Curr Opin Plant Biol. 2002;5(4):295–9.
40. Oeser B, Heidrich PM, Müller U, Tudzynski P, Tenberge KB. Polygalacturonase is a pathogenicity factor in the *Claviceps purpurea*/rye interaction. Fungal Genet Biol. 2002;36(3):176–86.
41. Rogers LM, Kim YK, Guo W, González-Candelas L, Li DX, Kolattukudy PE. Requirement for either a host-or pectin-induced pectate lyase for infection of *Pisum sativum* by *Nectria hematococca*. Proc Natl Acad Sci U S A. 2000;97(17):9813–8.
42. Isshiki A, Akimitsu K, Yamamoto M, Yamamoto H. Endopolygalacturonase is essential for citrus black rot caused by *Alternaria citri* but not brown spot caused by *Alternaria alternata*. Mol Plant Microbe In. 2001;14(6):749–57.
43. Deng LM, Huang X, Dao J, Xu YJ, Zhou KY, Wang WP, et al. Pectinesterase activity and gene expression correlate with pathogenesis of *Phytophthora infestans*. Front Plant Sci. 2024;15:1481165.
44. Fu L, Zhu CY, Ding XM, Yang XY, Morris PF, Tyler BM, et al. Characterization of cell-deathinducing members of the pectate lyase gene family in *Phytophthora capsici* and their contributions to infection of pepper. Mol Plant Microben. 2015;28(7):766–75.
45. Fry W. *Phytophthora infestans*: the plant (and R gene) destroyer. Mol Plant Pathol. 2008;9(3):385–402.
46. Gassmann W, Bhattachariee S. Effector-triggered immunity signaling: from gene-for-gene pathways to protein-protein interaction networks. Mol Plant Microbe In. 2012;25(7):862–8.
47. Waheed A, Wang YP, Nkurikiyimfura O, Li WY, Liu ST, Lurwanu Y, et al. Effector Avr4 in *Phytophthora infestans* escapes host immunity mainly through early termination. Front Microbiol. 2021;12:646062.
48. Wang ZW, Li TT, Zhang XJ, Feng JS, Liu ZT, Shan WX, et al. A *Phytophthora infestans* RXLR effector targets a potato ubiquitin-like domain-containing protein to inhibit the proteasome activity and hamper plant immunity. New Phytol. 2023;238:781–97.
49. Ballvora A, Ercolano MR, Weiss J, Meksem K, Bormann CA, Oberhagemann P, et al. The *R1* gene for potato resistance to late blight (*Phytophthora infestans*) belongs to the leucine Zipper/NBS/LRR class of plant resistance genes. Plant J. 2002;30(3):361–71.
50. Li GC, Huang SW, Guo X, Li Y, Yang Y, Guo Z, et al. Cloning and characterization of *R3b*; members of the *R3* superfamily of late blight resistance genes show sequence and functional divergence. Mol Plant Microbe In. 2011;24(10):1132–42.
51. Du J, Rietman H, Vleeshouwers VGAA. Agroinfiltration and PVX agroinfection in potato and *Nicotiana benthamiana*. J Vis Exp. 2014;83:e50971.
52. Li TT, Wang QH, Feng RR, Li LC, Ding LW, Fan GJ et al. Negative regulators of plant immunity derived from Cinnamyl alcohol dehydrogenases are targeted by multiple *Phytophthora* Avr3a-like effectors. New Phytol. 2019. https://doi.org/10.1111/nph.16139
53. Bos JIB, Armstrong MR, Gilroy EM, Boevink PC, Hein I, Taylor RM, et al. *Phytophthora infestans* effector AVR3a is essential for virulence and manipulates plant immunity by stabilizing host E3 ligase CMPG1. Proc Natl Acad Sci U S A. 2010;107(21):9909–14.
54. Chaparro-Garcia A, Schwizer S, Sklenar J, Yoshida K, Petre B, Bos JIB, et al. *Phytophthora infestans* RXLR-WY effector AVR3a associates with Dynamin-related protein 2 required for endocytosis of the plant pattern recognition receptor FLS2. PLoS ONE. 2015;10(9):e0137071.

55. Lee H, Park M, Kweon Y, Lee D, Shin C. Targeted dsRNA-mediated suppression of *Phytophthora infestans* infection via Avr3a. Appl Biol Chem. 2024;67(1):97.

Publisher's note